Available online at www.sciencedirect.com
ScienceDirect
Journal of Sound and Vibration 325 (2009) 382–396
JOURNAL OF SOUND AND VIBRATION
www.elsevier.com/locate/jsvi

Semi-analytic solutions to nonlinear vibrations of microbeams under suddenly applied voltages

M. Moghimi Zand[a,*], M.T. Ahmadian[b,*], B. Rashidian[c]

[a]School of Mechanical Engineering, Sharif University of Technology, Tehran, Iran
[b]Center of Excellence in Design, Robotics and Automation, School of Mechanical Engineering, Sharif University of Technology, Tehran, Iran
[c]School of Electrical Engineering, Sharif University of Technology, Tehran, Iran

Received 26 May 2008; received in revised form 3 February 2009; accepted 12 March 2009
Handling Editor: M.P. Cartmell
Available online 20 May 2009

Abstract

In this study, nonlinear oscillations of microbeams, actuated by suddenly applied electrostatic force, are investigated. Effects of electrostatic actuation, residual stress, midplane stretching and fringing fields are considered in modeling. Galerkin's decomposition method is utilized to convert the governing nonlinear partial differential equation to a nonlinear ordinary differential equation. Homotopy analysis method is used to find semi-analytic solutions to the vibrations of microbeams. Convergence regions of the solution series are determined. Influences of increasing the voltage and midplane stretching on the frequency of vibrations are also studied. Results are in good agreement with numerical and experimental findings.

1. Introduction

A microbeam, actuated by electrostatic distributed force, is a flexible beam-shaped element attached to a fixed rigid substrate. Electrostatically actuated microbeams are extensively used in different applications such as signal filtering and mass sensing [1]. When the input voltage exceeds a critical value, called pull-in voltage (V_{pi}), the flexible microbeam spontaneously deflects towards the rigid plate. In microbeams, pull-in instability is a basic phenomenon considered in design. Pull-in instability was observed experimentally by Taylor [2] and Nathanson et al. [3]. Osterberg studied microelectromechanical systems (MEMS) with circular and rectangular shapes and achieved several closed-form models for pull-in instability in these systems [4].

When the rate of voltage variation is low and consequently inertia has almost no influence on the microsystem behavior, the critical value of voltage is called static pull-in voltage (V_{pi}). However, when the rate of voltage variation is not negligible, the effect of inertia has to be considered and the critical voltage value is called dynamic pull-in voltage (V_{pid}). The pull-in instability related to this situation is called dynamic pull-in instability [5,6].

*Corresponding authors. Tel.: +98 21 66165503; fax: +98 21 66000021.
E-mail addresses: moghimizand@mech.sharif.edu (M. Moghimi Zand), ahmadian@sharif.edu (M.T. Ahmadian).

0022-460X/$ - see front matter © 2009 Elsevier Ltd. All rights reserved.
doi:10.1016/j.jsv.2009.03.023

Nomenclature

b	width of the plate
d_0	initial air gap
E_y	effective Young's modulus
h	plate thickness
I_b	moment of inertia of the cross-section
l	length of the plate
m	degree of the electrostatic force Taylor approximation
N_i	initial (residual) axial load
N_s	axial load due to the midplane stretching
p	order of approximation
q	embedding parameter
t	time
$u(t)$	time-dependent deflection parameter
V	voltage
Z	deflection

Greek symbols

ε	vacuum permittivity
ρ	density
$\varphi(x)$	trial function
ω	nonlinear frequency

Special functions and parameters

$\hbar$	auxiliary parameter
H	homotopy function
$\mathfrak{L}$	auxiliary linear operator
$\mathfrak{N}$	nonlinear operator

Studying vibrational behavior of MEMS is quite useful in determining design parameters of these systems. Vibrational characteristics of microbeams have been generally studied assuming small vibrations around a deflected position. In Ref. [7], oscillatory behavior of microbeams considering midplane stretching has been studied. In Ref. [1] vibrations of double-clamped microbeams, predeformed by an electric field, have been investigated. Vibrations of electrostatically actuated microstructures have also been studied in Refs. [8–10].

Different techniques have been proposed for finding solutions to nonlinear equations of MEMS, for example the differential quadrature method [11], the finite element method [9,10] and homotopy methods [12]. Although it is difficult to get an analytic approximation for different phenomena in MEMS, there are some analytic methods for nonlinear problems of microelectromechanical systems such as perturbation techniques [13,14]. In general, perturbation approximations are valid only for weakly nonlinear problems [15]. Based on the homotopy method in topology, Liao proposed homotopy analysis method (HAM) to present analytic solutions to strongly nonlinear problems [15]. This method can also be effective in finding solutions to the vibrations of microbeams.

In the present paper, vibrations of microbeams subjected to suddenly applied step voltages are investigated. Different sources of nonlinearity such as electrostatic force and midplane stretching are considered. Galerkin's decomposition method is utilized to convert the nonlinear partial differential equation of motion to a nonlinear ordinary differential equation. Afterward, Liao's homotopy analysis method is utilized to find semi-analytic solutions to the nonlinear vibrations of microbeams. Effects of increasing voltage, midplane stretching and fringing fields are studied. Influences of different parameters on convergence regions are also investigated.

2. Modeling and formulation

Fig. 1 displays a prismatic double-clamped microbeam suspended above a rigid substrate. When a voltage V is applied between the conductive microbeam and the substrate plate, an attractive electrostatic force causes the microbeam to deflect. In Fig. 1, x is the coordinate along the length, z is the coordinate along the thickness, Z is deflection in the z-direction and t is the time. The length of the microbeam is l, the width is b, the density is ρ, the thickness is h, the vacuum permittivity is ε, the moment of inertia of the cross-section about the y-axis is I_b, the effective Young's modulus of the beam is E_y and the air initial gap is d_0.

The electrostatic force per unit area takes the following form:

$$F_e = 1/2\frac{\varepsilon V^2}{(d_0 - Z(x,t))^2}\left(1 + \beta\frac{d_0 - Z(x,t)}{b}\right) \tag{1}$$

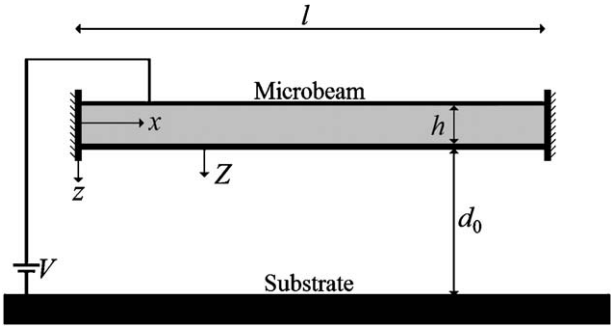

Fig. 1. Schematic view of a double-clamped microbeam.

Here the term β accounts for the fringing fields effect due to the finite width of the beam. For a double-clamped beam $\beta = 0.65$.

By incorporating von Kármán nonlinearity for midplane stretching, the deflection Z in z-direction is governed by [1]

$$\rho bh\frac{\partial^2 Z}{\partial t^2} + E_y I_b \frac{\partial^4 Z}{\partial x^4} - (N_i + N_s)\frac{\partial^2 Z}{\partial x^2} - bF_e = 0 \tag{2}$$

where N_i is the residual (initial) axial load and N_s the axial load due to the midplane stretching which is given by

$$N_s = \frac{E_y bh}{2l}\int_0^l \left(\frac{\partial Z}{\partial x}\right)^2 \mathrm{d}x \tag{3}$$

The microbeam deflection is subjected to the following kinematic boundary conditions:

$$Z(0,t) = 0, \quad \frac{\partial Z(0,t)}{\partial x} = 0, \quad Z(l,t) = 0, \quad \frac{\partial Z(l,t)}{\partial x} = 0 \tag{4}$$

The initial conditions are as follows:

$$Z(x,0) = 0, \quad \frac{\partial Z(x,0)}{\partial t} = 0 \tag{5}$$

Based on one DOF model of the beams, Eqs. (2)–(5) can be solved by appropriate accuracy [1]. The solution is constructed by expressing the deflection function as the product of two separate functions

$$Z(x,t) = \phi(x)u(t) \tag{6}$$

where $u(t)$ is an unknown time-dependent deflection parameter and $\phi(x)$ is a trial function satisfying the kinematic boundary conditions. For example, $\phi(x)$ can be assumed as

$$\phi(x) = \left(\frac{x}{l}\right)^2\left(1 - \frac{x}{l}\right)^2 \tag{7}$$

The term F_e in Eq. (2) can be approximated by Taylor's series as

$$\begin{aligned} F_e &= \frac{1}{2}\frac{\varepsilon V^2}{(d_0 - Z(x,t))^2}\left(1 + \beta\frac{d_0 - Z(x,t)}{b}\right) = \sum_{j=0}^{m}\eta_j Z(x,t)^j \\ &= \frac{1}{2}\varepsilon V^2\left(\frac{1}{d_0^2} + \frac{2Z(x,t)}{d_0^3} + \frac{3Z(x,t)^2}{d_0^4} + \frac{4Z(x,t)^3}{d_0^5} + \frac{5Z(x,t)^4}{d_0^6} + \cdots\right) \\ &\quad + \frac{1}{2}\frac{\varepsilon\beta V^2}{b}\left(\frac{1}{d_0} + \frac{Z(x,t)}{d_0^2} + \frac{Z(x,t)^2}{d_0^3} + \frac{Z(x,t)^3}{d_0^4} + \frac{Z(x,t)^4}{d_0^5} + \cdots\right) \end{aligned} \tag{8}$$

where m is the degree of the electrostatic force Taylor approximation. Substituting for F_e from Eq. (8) into Eq. (2) and also for N_s from Eq. (3) into Eq. (2), one obtains

$$T(Z(x,t)) = \rho bh\frac{\partial^2 Z(x,t)}{\partial t^2} + E_y I_b \frac{\partial^4 Z(x,t)}{\partial x^4} - \left(N_i + \frac{E_y bh}{2l}\int_0^l \left(\frac{\partial Z(x,t)}{\partial x}\right)^2 \mathrm{d}x\right)\frac{\partial^2 Z(x,t)}{\partial x^2} - \frac{b\varepsilon V^2}{2}\left(\frac{1}{d_0^2} + \frac{2Z(x,t)}{d_0^3} + \frac{3Z(x,t)^2}{d_0^4} + \frac{4Z(x,t)^3}{d_0^5} + \frac{5Z(x,t)^4}{d_0^6} + \cdots\right) - \frac{\beta\varepsilon V^2}{2}\left(\frac{1}{d_0} + \frac{Z(x,t)}{d_0^2} + \frac{Z(x,t)^2}{d_0^3} + \frac{Z(x,t)^3}{d_0^4} + \frac{Z(x,t)^4}{d_0^5} + \cdots\right) = 0 \tag{9}$$

The one-parameter Galerkin's solution can be computed by [1]

$$\int_0^l \phi(x)T(Z(x,t))\,\mathrm{d}x = 0 \tag{10}$$

After substituting for $T(Z(x,\ t))$ from Eq. (9) into Eq. (10) and integrating by parts in some terms, the governing equation for $u(t)$ becomes (for the case $m = 4$)

$$M\frac{\mathrm{d}^2}{\mathrm{d}t^2}u(t) + M\lambda u(t) + LV^2 + DV^2u^2(t) + (S + EV^2)u^3(t) + GV^2u^4(t) = 0 \tag{11}$$

where

$$\lambda = \frac{K - V^2B}{M} \tag{12}$$

For more accuracy, higher degrees of the electrostatic force Taylor approximation can be used. For the cases $m = 5$ and 6, one obtains the following equations, respectively:

$$M\frac{\mathrm{d}^2}{\mathrm{d}t^2}u(t) + M\lambda u(t) + LV^2 + DV^2u^2(t) + (S + EV^2)u^3(t) + GV^2u^4(t) + JV^2u^5(t) = 0 \tag{13}$$

$$M\frac{\mathrm{d}^2}{\mathrm{d}t^2}u(t) + M\lambda u(t) + LV^2 + DV^2u^2(t) + (S + EV^2)u^3(t) + GV^2u^4(t) + JV^2u^5(t) + PV^2u^6(t) = 0 \tag{14}$$

subject to zero initial conditions. Coefficients M, K, L, D, S, E, G, J, P and B are presented in Appendix A. In the next section, homotopy analysis method is utilized to solve the microbeam problem.

3. Application of homotopy analysis method to the microbeam problem

HAM is an effective analytic method for solving nonlinear equations. This method transforms a general nonlinear problem into an infinite number of linear problems by embedding an auxiliary parameter q [16]. As q increases from 0 to 1, the solution varies from the initial approximation to the exact solution. The homotopy function is constructed as [15–21]

$$\mathrm{H}(\Phi; q, \hbar, H(t)) = (1-q)\mathfrak{L}[\Phi(t;q) - u_0(t)] - q\hbar H(t)\mathfrak{N}[\Phi(t;q)] \tag{15}$$

where $\hbar$, $u_0(t)$, $H(t)$, $\mathfrak{L}$ and $\mathfrak{N}$ are a nonzero auxiliary parameter, an initial guess, a nonzero auxiliary function, an auxiliary linear operator and a nonlinear operator, respectively. Quantities $\hbar$ and $H(t)$ adjust the convergence region of the solution. For the microbeam problem, the auxiliary function can be chosen in the form $H(t) = 1$.

Consider Eq. (11) as the equation of motion ($m = 4$). The procedures for the cases $m = 5$ and 6 are similar to the case $m = 4$. From Eq. (11), the nonlinear operator $\mathfrak{N}[\Phi(t;q), \Lambda(q)]$ can be defined as

$$\mathfrak{N}[\Phi(t;q), \Lambda(q)] = \frac{\partial^2\Phi(t;q)}{\partial t^2} + \Lambda(q)\Phi(t;q) + \frac{LV^2 + DV^2\Phi^2(t;q) + (S + EV^2)\Phi^3(t;q) + GV^2\Phi^4(t;q)}{M} = 0 \tag{16}$$

subject to zero initial conditions. It should be noted that $\Lambda(1) = \lambda = (K - BV^2)/M$.

To construct the homotopy function, the auxiliary linear operator can be chosen as

$$\mathfrak{L}[\Phi(t;q)] = \frac{\partial^2 \Phi(t;q)}{\partial t^2} + \omega^2 \Phi(t;q) \tag{17}$$

The function $\Phi(t;q)$ can be expanded in a power series of the embedding parameter q using Taylor's theorem as follows:

$$\Phi(t;q) = u_0(t) + qu_1(t) + q^2u_2(t) + q^3u_3(t) + q^4u_4(t) + q^5u_5(t) + q^6u_6(t) + \cdots \tag{18}$$

The function Λ can be expanded as

$$\Lambda(q) = \omega^2 + q\omega_1(\omega) + q^2\omega_2(\omega) + q^3\omega_3(\omega) + q^4\omega_4(\omega) + \cdots \tag{19}$$

By equating to zero the homotopy function, the zero-order deformation equation is constructed as

$$(1-q)\mathfrak{L}[\Phi(t;q) - u_0(t)] = q\hbar\mathfrak{N}[\Phi(t;q), \Lambda(q)] \tag{20}$$

$$\Phi(0;q) = 0, \quad \frac{\partial \Phi(0;q)}{\partial t} = 0 \tag{21}$$

When $q = 0$, Eq. (20) becomes

$$\mathfrak{L}[\Phi(t;0) - u_0(t)] = 0 \tag{22}$$

which gives the zero-order approximation of $u(t)$.

It is straightforward to set the initial guess $u_0(t)$ to zero. Differentiating Eq. (20) with respect to q and then setting $q = 0$, yields the first-order deformation equation, which gives the first-order approximation of $u(t)$ by solving

$$\mathfrak{L}[u_1(t)] = \hbar\mathfrak{N}[\Phi(t;q), \Lambda(q)]\big|_{q=0} \tag{23}$$

subject to zero initial conditions. The higher-order approximations of the solution $u(t)$ can be found by solving high-order deformation equations. Differentiating Eq. (20) j times with respect to q, and then setting $q = 0$ and finally dividing each side by $j!$, one obtains the jth-order deformation equation

$$\mathfrak{L}[u_j(t) - \chi_j u_{j-1}(t)] = \frac{1}{(j-1)!}\hbar\frac{\partial^{j-1}\mathfrak{N}[\Phi(t;q), \Lambda(q)]}{\partial q^{j-1}}\bigg|_{q=0} \tag{24}$$

where

$$\chi_j = \begin{cases} 0 & \text{when } j \leqslant 1, \\ 1 & \text{otherwise.} \end{cases} \quad \text{and} \quad \Lambda(q) = \omega^2 + q\omega_1(\omega) + q^2\omega_2(\omega) + q^3\omega_3(\omega) + q^4\omega_4(\omega) + \cdots \tag{25}$$

Here, the terms ω_j can be identified by means of no secular terms. It is noteworthy that the vibrations of an undamped microbeam under the actuation of the electrostatic force can be expressed by the following base functions:

$$\cos(k\omega t), \quad k = 1, 2, 3, \ldots \tag{26}$$

Therefore, to eliminate the secular terms in the jth-order approximation, one can set the coefficient of $\cos(\omega t)$ in the $(j-1)$th-order deformation equation to zero. This provides an algebraic equation. Solving this algebraic equation yields ω_{j-2} as a function of ω. After finding sufficient approximations, by setting $q = 1$ in Eqs. (18) and (19), one gets

$$\Lambda(1) = \lambda = \omega^2 + \sum_{j=1}^{p} \omega_k(\omega) = \omega^2 + \omega_1(\omega) + \omega_2(\omega) + \cdots + \omega_p(\omega) \tag{27}$$

$$u(t) = \sum_{j=0}^{p+2} u_j(t) = u_0(t) + u_1(t) + u_2(t) + u_3(t) + u_4(t) + \cdots + u_{p+2}(t) \tag{28}$$

where p is the order of approximation. The nonlinear frequency ω can be found by solving Eq. (27). The method can also be applied for different degrees of the electrostatic force Taylor approximation (m). The terms ω_1, ω_2, ω_3, ω_4, ω_5 and ω_6 for $m = 4$ are presented in Appendix B.

Table 1
The parameters of the double-clamped microbeams [22].

Beam length (μm)	Thickness (μm)	Initial gap (μm)	Width (μm)	Residual axial load (N)	Effective Young's modulus (GPa)
210 310 410 510	1.5	1.18	100	0.0009 (tensile)	166

Table 2
A comparison between the experimental and calculated results.

Beam length (μm)	$\omega_0/2\pi$ (kHz)			
	Measured [22]	Calculated [22]	Calculated [11]	Semi-analytic method (present study, $m = 4$)
210	322.05	324.70	324.70	324.78
310	163.22	164.35	163.46	163.16
410	102.17	103.80	103.70	103.42
510	73.79	74.80	73.46	74.38

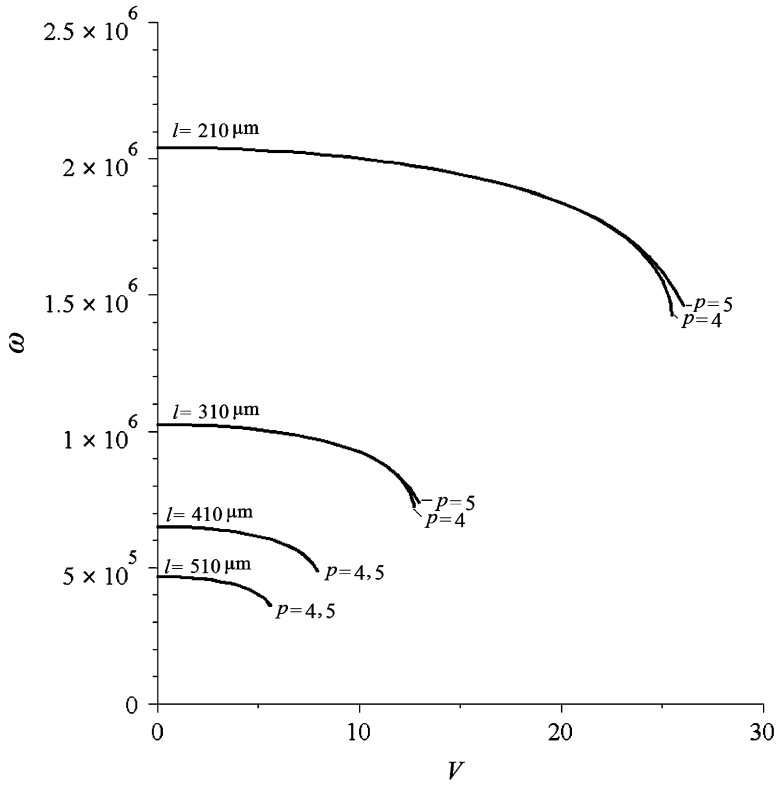

Fig. 2. Variations of the nonlinear frequency (Hz) with applied step voltage (V) for different values of p ($m = 4$).

4. Results and discussions

To validate the model, a comparison is performed using microbeams with parameters listed in Table 1. The effective Young's modulus for the microbeams material is $E_y = 166\,\text{GPa}$. Further, it is assumed that the residual axial load is $N_i = 0.0009\,\text{N}$ (residual stress $\sigma = 6\,\text{MPa}$). The residual stress may be induced during the fabrication process. Table 2 lists the calculated and measured initial frequencies for these microbeams. Table 2 reveals that the results obtained from the present model agree very well with numerical and experimental results presented in the literature.

Fig. 2 shows variations of nonlinear frequency versus applied voltage using semi-analytic method for $m = 4$ and 5. As it can be seen, when the input voltage increases, the nonlinear frequency of vibrations decreases. This diagram signifies that for a large range of applied voltages, there exists good agreement between results calculated by assuming $m = 4$ and those obtained by assuming $m = 5$.

In Fig. 3 variation of the nonlinear frequency with the input voltage for various degrees of electrostatic force approximation is shown. The presented diagram reveals that the differences between nonlinear frequencies computed by fourth, fifth and sixth degree approximations are negligible. It indicates that the fourth degree approximation for electrostatic force is sufficient in calculations for these microbeams.

Fig. 4a shows deflections of the double-clamped microbeam with length $l = 210\,\mu\text{m}$ for input voltage of 20 V. Fig. 4b depicts deflections for input voltage of 25 V. As seen, for low voltages, low orders of approximation (p) are sufficient to find deflections accurately. Nevertheless, for high voltages, higher orders of approximation are required. In these figures, the microbeam equation has been solved numerically by Runge–Kutta method using MAPLE *fsolve* command. It is noteworthy that expanding Λ using Eq. (19) effectively reduces the required order of approximation (p); however, it forces us to solve a set of nonlinear equations to find the nonlinear frequency. A method of finding the frequency without a need for solving nonlinear equations has been presented in [23].

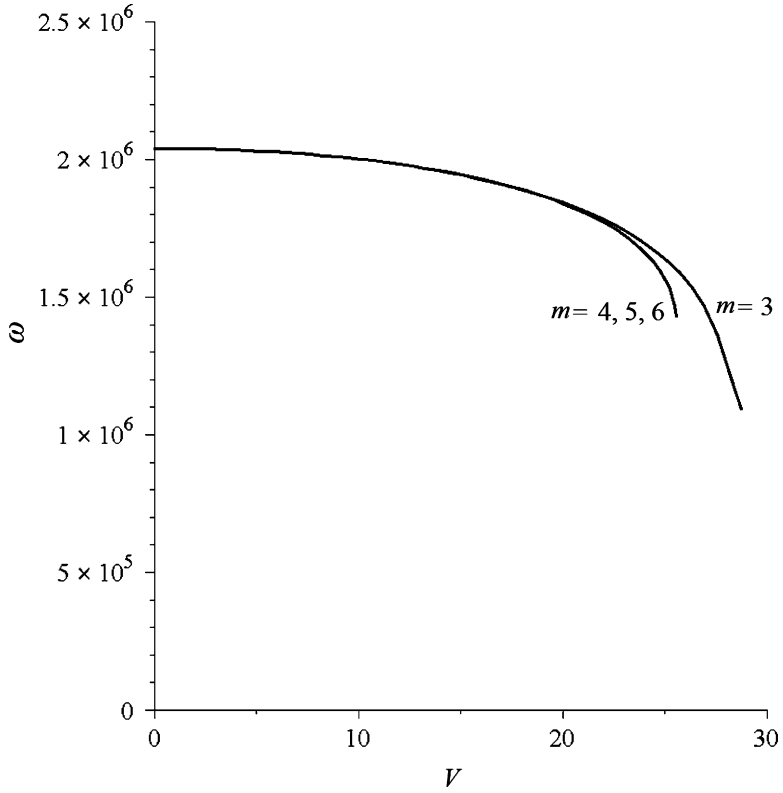

Fig. 3. Variations of the nonlinear frequency (Hz) with applied step voltage (V) for the double-clamped microbeam with length $l = 210\,\mu\text{m}$ and different values of m ($p = 3$).

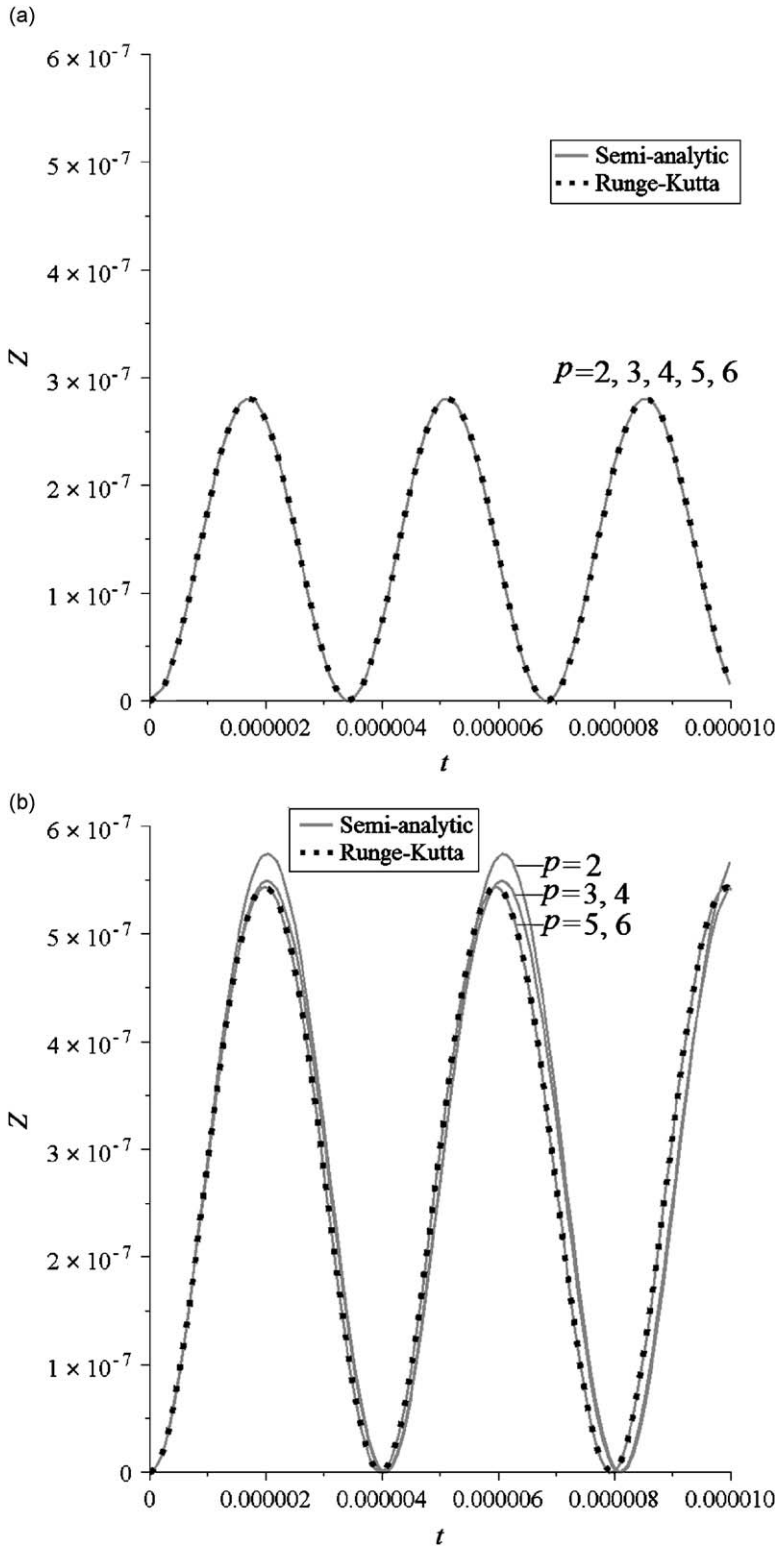

Fig. 4. Midpoint deflection time history for the double-clamped microbeam with length $l = 210\,\mu m$: (a) input voltage of 20 V and (b) input voltage of 25 V ($V_{pid} = 26.96$ V). ● Runge–Kutta; — Semi-analytic.

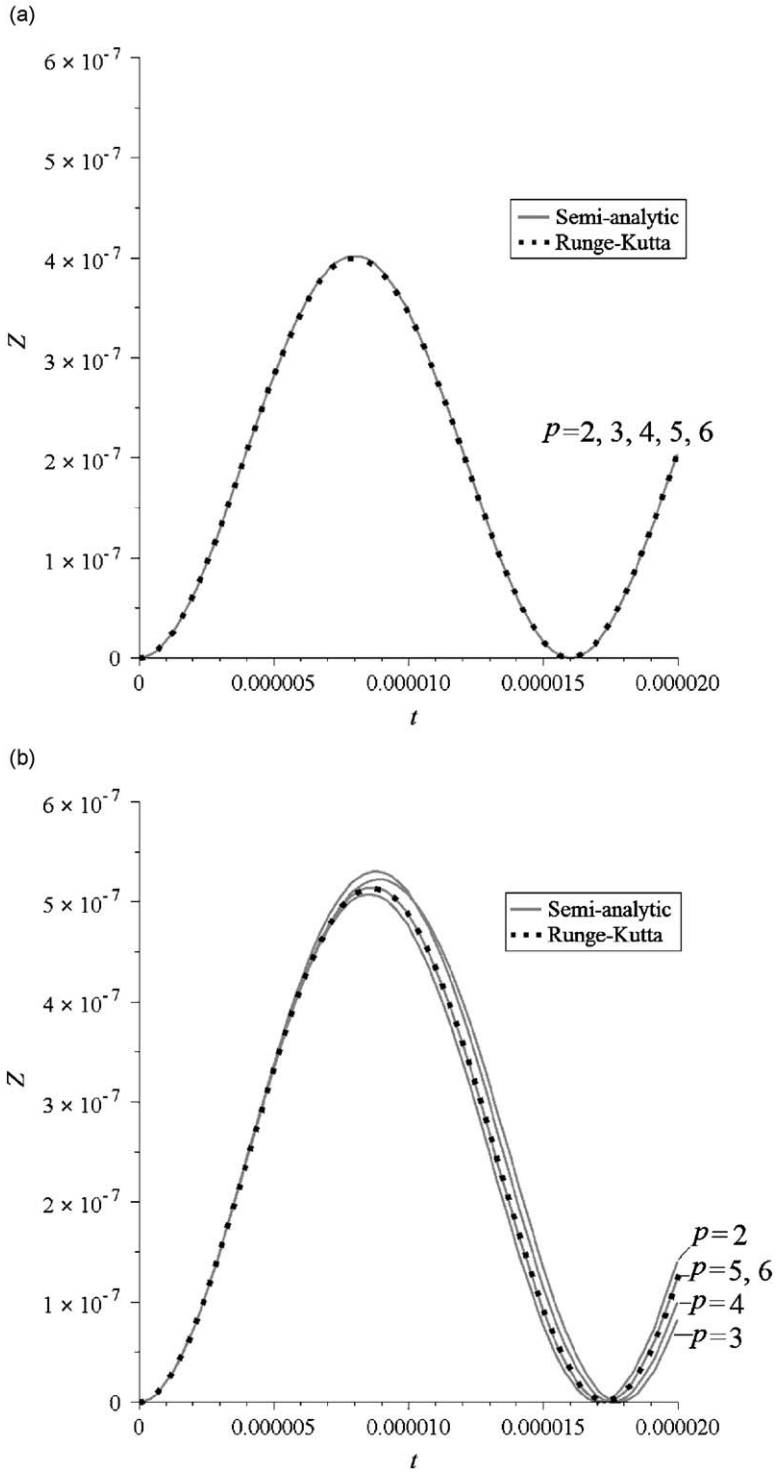

Fig. 5. Midpoint deflection time history for the double-clamped microbeam with length $l = 510\,\mu m$: (a) input voltage of 5.2 V and (b) input voltage of 5.6 V ($V_{pid} = 6.04$ V). ● Runge–Kutta; — Semi-analytic.

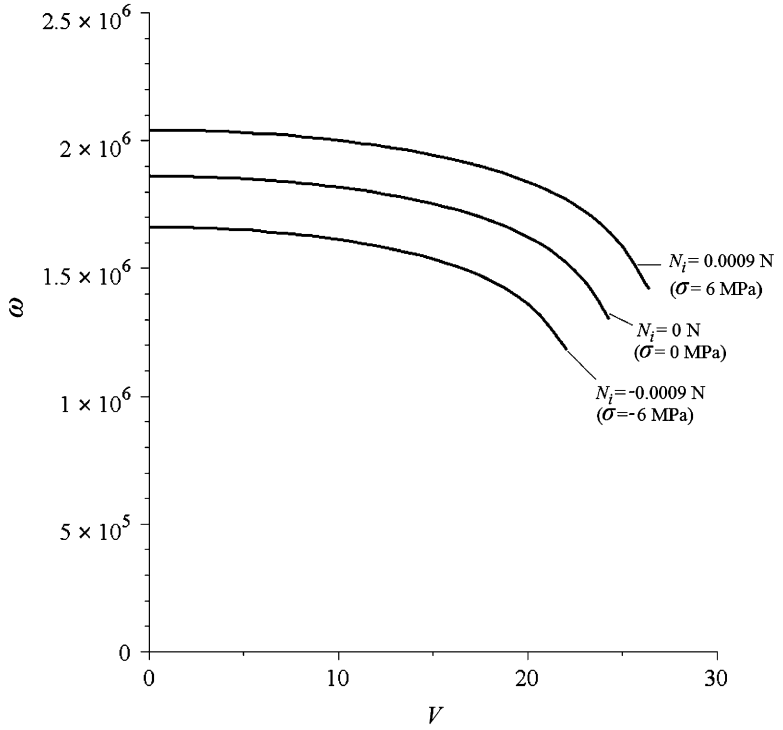

Fig. 6. Variations of the nonlinear frequency (Hz) with applied step voltage (V) for the double-clamped microbeam with length $l = 210\,\mu m$ and different residual axial loads.

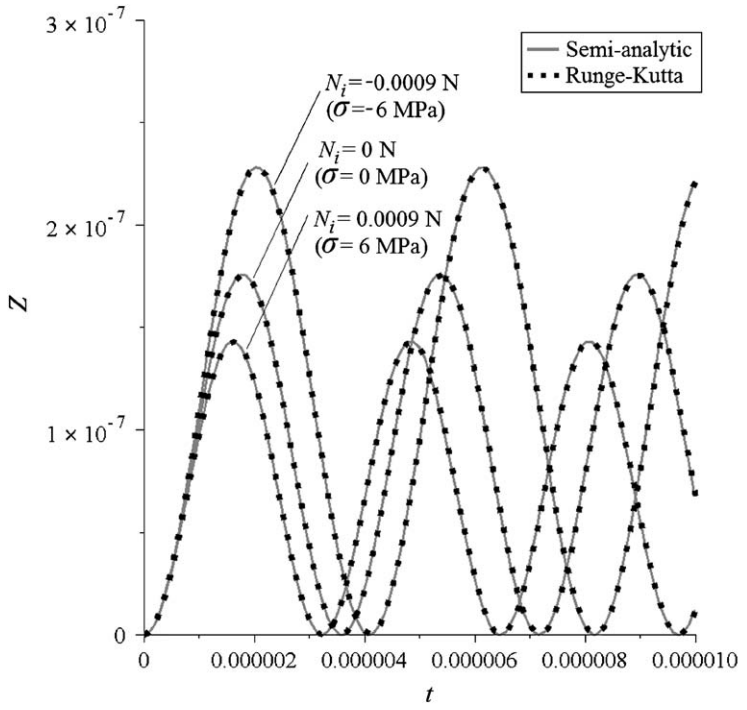

Fig. 7. Midpoint deflection time history for the double-clamped microbeam with length $l = 210\,\mu m$ and different residual axial loads actuated by input voltage of 15 V.● Runge–Kutta; — Semi-analytic.

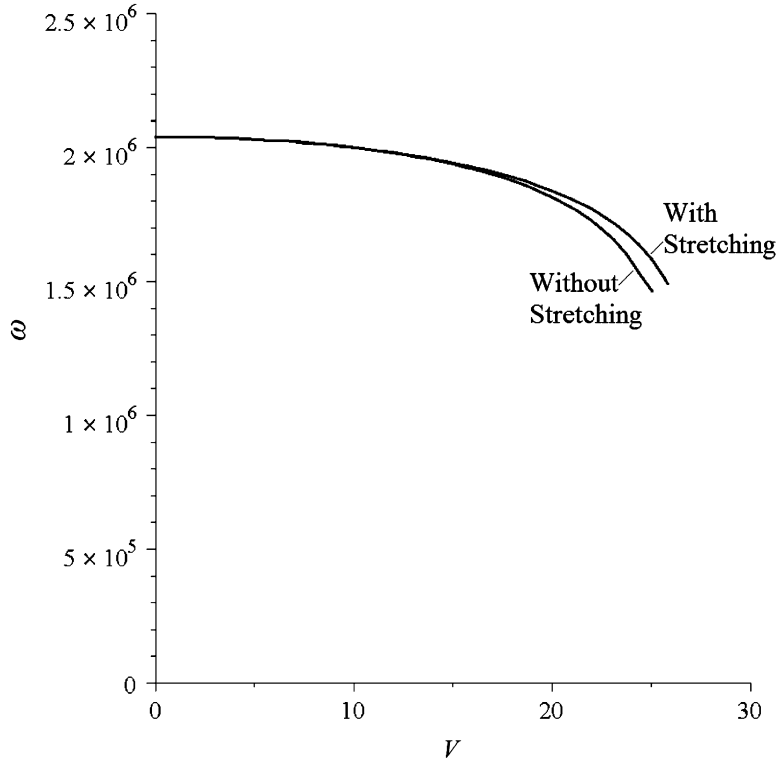

Fig. 8. Variations of the nonlinear frequency (Hz) with applied step voltage (V) for the double-clamped microbeam with length $l = 210\,\mu m$ with and without midplane stretching.

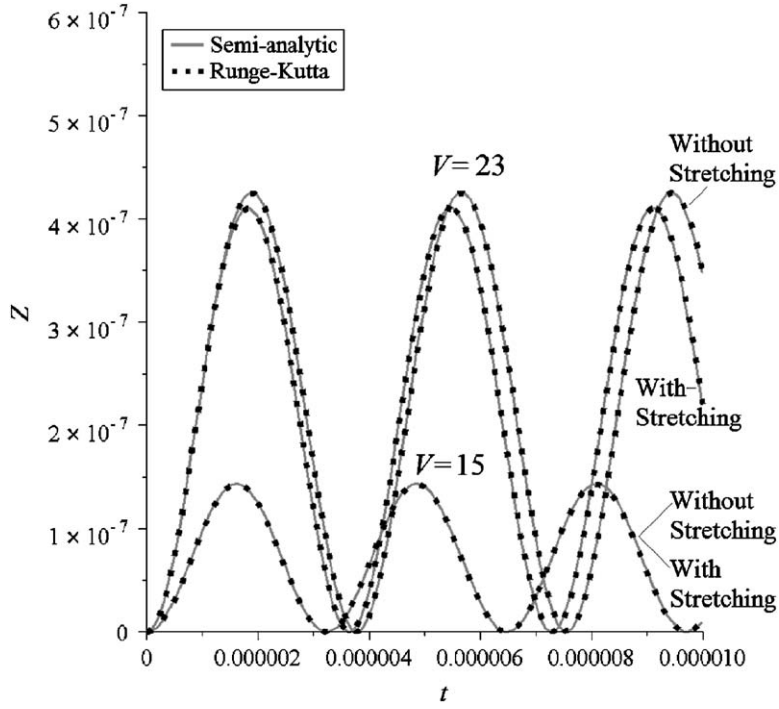

Fig. 9. Midpoint deflection time history for the double-clamped microbeam with length $l = 210\,\mu m$ ($p = 6$, $m = 4$). ● Runge–Kutta; — Semi-analytic.

Figs. 5a and b show deflection time history of a microbeam with length $l = 510\,\mu m$ for input voltages of 5.2 and 5.6 V, respectively. It can be observed from Figs. 4 and 5 that there is excellent agreement between results calculated by Runge–Kutta method and those obtained by the semi-analytic method (particularly for $p = 5, 6$).

In Fig. 6 influence of residual stress on nonlinear frequency is observed. As it can be seen, pretension in microbeams results in increasing nonlinear frequency.

Fig. 7 elaborates deflection time history of the microbeam with length 210 μm for different axial loads. As depicted in Fig. 7, precompression increases deflections for a specific applied voltage.

In Fig. 8 influence of the midplane stretching on the nonlinear frequency is depicted. As it can be seen, accounting for the midplane stretching decreases the amplitudes of vibrations. On the other hand, the neglecting of the midplane stretching underestimates the microbeam stiffness and nonlinear frequency.

Fig. 9 shows deflection time history of the microbeam with length $l = 210\,\mu m$ for low (15 V) and high (23 V) voltages. It can be seen that midplane stretching has a relatively significant effect on deflections for high voltages; while for low voltages, the effect is negligible.

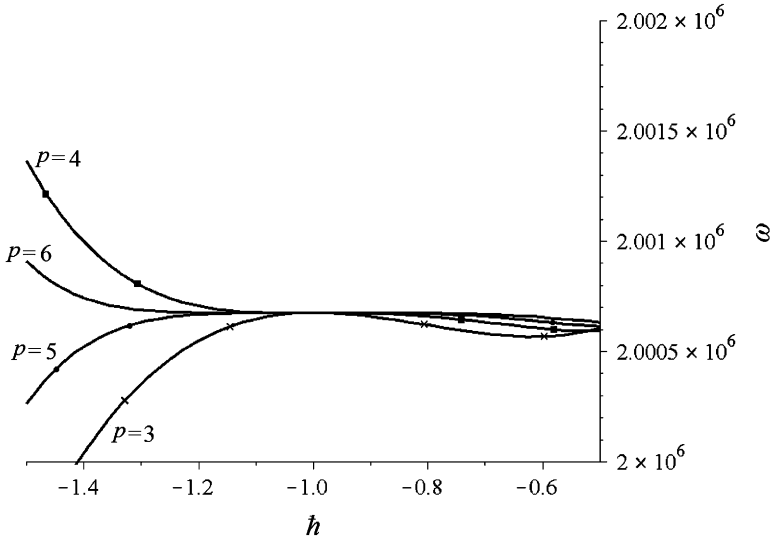

Fig. 10. The $\hbar$-curve of ω for the microbeam with length $l = 210\,\mu m$ actuated by a 10 V step-input voltage.

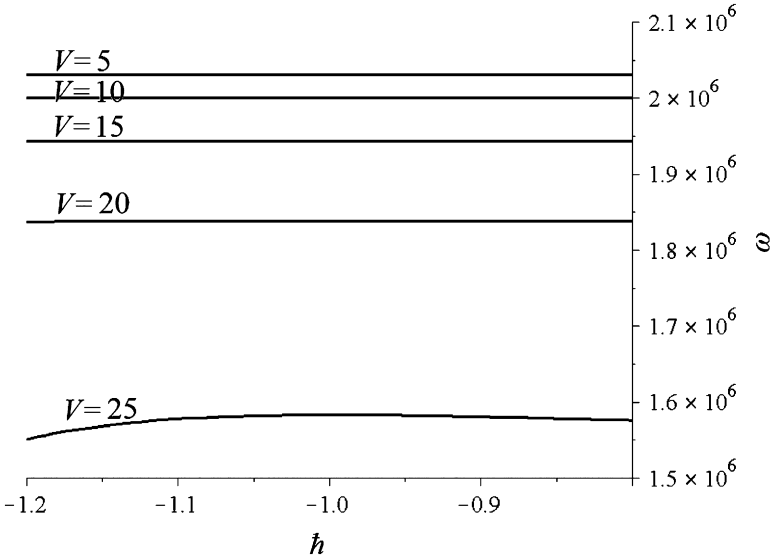

Fig. 11. The $\hbar$-curve of ω for the microbeam with length $l = 210\,\mu m$ actuated by different voltages ($p = 6$).

As discussed before, there is clearly excellent agreement between numerical results calculated by Runge–Kutta method and semi-analytic results for $p = 5$, 6 in diagrams containing midpoint deflection time history.

In homotopy analysis method, by plotting $\hbar$-curves, it is easy to find a proper value of $\hbar$ to ensure that the solution series converge [16]. These curves ($\hbar$-curves) depict variations of solutions with $\hbar$. The convergence region and rate of the solution series can be adjusted by means of the auxiliary parameter $\hbar$. A proper solution series has to be independent upon the auxiliary parameter $\hbar$. In Fig. 10 the $\hbar$-curve of ω for the microbeam with length $l = 210\,\mu\text{m}$ is depicted. The microbeam is actuated by a step voltage of 10 V. As it can be seen, using the higher orders of approximation (p) enlarges convergence regions of the solution series.

In Fig. 11 the $\hbar$-curve of ω for the above-mentioned microbeam is shown for different voltages. Order of approximation (p) is equal to 6 for this figure. It can be deduced from Fig. 11 that decreasing the input voltage enlarges convergence regions.

5. Conclusion

In this research, homotopy analysis method has been utilized to find semi-analytic solutions to nonlinear oscillations of microbeams, actuated by step input voltages. The nonlinear ordinary differential equation of motion has been built using the Galerkin's decomposition method. The equation of motion has been solved by homotopy analysis method. Influences of increasing voltage, axial load and midplane stretching on nonlinear vibrations have been investigated. It was shown that by increasing actuation voltage, higher-order approximations are required to find deflections accurately. Effect of auxiliary parameter on solutions has also been considered to determine convergence regions. Results indicate that higher orders of approximation enlarge convergence regions of the solution series. Comparing the results of the semi-analytic method with the numerical results shows excellent agreement between them.

Acknowledgment

The authors would like to thank Professor Shijun Liao for his valuable suggestions.

Appendix A

$$M = \int_0^l \rho bh\phi(x)^2\,\mathrm{d}x, \quad L = -\int_0^l \left(\frac{0.5\varepsilon b\phi(x)}{d_0^2} + \frac{0.5\varepsilon\beta\phi(x)}{d_0}\right)\mathrm{d}x$$

$$B = -\int_0^l \left(\frac{\varepsilon b\phi(x)^2}{d_0^3} + \frac{0.5\varepsilon\beta\phi(x)^2}{d_0^2}\right)\mathrm{d}x, \quad D = -\int_0^l \left(\frac{1.5\varepsilon b\phi(x)^3}{d_0^4} + \frac{0.5\varepsilon\beta\phi(x)^3}{d_0^3}\right)\mathrm{d}x$$

$$E = -\int_0^l \left(\frac{2\varepsilon b\phi(x)^4}{d_0^5} + \frac{0.5\varepsilon\beta\phi(x)^4}{d_0^4}\right)\mathrm{d}x, \quad G = -\int_0^l \left(\frac{2.5\varepsilon b\phi(x)^5}{d_0^6} + \frac{0.5\varepsilon\beta\phi(x)^5}{d_0^5}\right)\mathrm{d}x$$

$$J = -\int_0^l \left(\frac{3\varepsilon b\phi(x)^6}{d_0^7} + \frac{0.5\varepsilon\beta\phi(x)^6}{d_0^6}\right)\mathrm{d}x, \quad P = -\int_0^l \left(\frac{3.5\varepsilon b\phi(x)^7}{d_0^8} + \frac{0.5\varepsilon\beta\phi(x)^7}{d_0^7}\right)\mathrm{d}x$$

$$K = \int_0^l \left(E_y I_b\phi(x)\frac{\mathrm{d}^4\phi(x)}{\mathrm{d}x^4} - N_i\phi(x)\frac{\mathrm{d}^2\phi(x)}{\mathrm{d}x^2}\right)\mathrm{d}x, \quad S = -\int_0^l \frac{0.5E_y bh}{l}\phi(x)\frac{\mathrm{d}^2\phi(x)}{\mathrm{d}x^2}\left(\int_0^l \left(\frac{\mathrm{d}\phi(x)}{\mathrm{d}x}\right)^2\mathrm{d}x\right)\mathrm{d}x$$

Appendix B

$$\omega_1 = -\frac{2\hbar LV^4 D}{M^2\omega^2}$$

$$\omega_2 = -\frac{\hbar LV^4}{4M^3\omega^4}(8\hbar DM\omega^2 + 8DM\omega^2 + 15\hbar LS + 15\hbar LEV^2)$$

$$\begin{aligned}\omega_3 = \frac{\hbar LV^4}{6M^4\omega^6}(&-42\hbar^2L^2GV^4 - 45M\hbar LE\omega^2V^2 - 45M\hbar^2LE\omega^2V^2 - 12M^2\hbar^2D\omega^4\\ &- 45M\hbar LS\omega^2 - 45M\hbar^2LS\omega^2 + 7\hbar^2LD^2V^4 - 12DM^2\omega^4 - 24\hbar DM^2\omega^4)\end{aligned}$$

$$\begin{aligned}\omega_4 = \frac{\hbar LV^4}{4M^5\omega^8}(&-90M^2\omega^4\hbar^2LEV^2 - 84M\omega^2\hbar^2L^2GV^4 - 8M^3D\omega^6 - 45M^2\hbar LS\omega^4\\ &+ 14M\hbar^3LD^2\omega^2V^4 + 30L^2\hbar^3DSV^4 - 24M^3\hbar D\omega^6 - 45M^2\hbar^3LE\omega^4V^2\\ &- 84M\omega^2\hbar^3L^2GV^4 - 45M^2\hbar^3LS\omega^4 - 24M^3\hbar^2D\omega^6 - 45\hbar LEM^2\omega^4V^2\\ &+ 14M\hbar^2LD^2\omega^2V^4 - 8M^3\hbar^3D\omega^6 - 90M^2\hbar^2LS\omega^4 + 30\hbar^3L^2DEV^6)\end{aligned}$$

$$\begin{aligned}\omega_5 = -\frac{\hbar LV^4}{1152M^6\omega^{10}}(&-13365\hbar^4L^3V^4S^2 - 34560M\omega^2\hbar^4L^2DEV^6 - 8064\hbar^4LV^4M^2D^2\omega^4\\ &+ 1408\hbar^4L^2V^8D^3 + 17280\hbar^4LSM^3\omega^6 + 48384L^2\hbar^4GM^2V^4\omega^4 - 34560L^2\hbar^4SMDV^4\omega^2\\ &+ 17280\hbar^4LEM^3\omega^6 - 26730L^3\hbar^4ESV^6 - 22176L^3\hbar^4DGV^8 - 8064L\hbar^2M^2D^2V^4\omega^4\\ &+ 2304\hbar^4M^4D\omega^8 - 13365\hbar^4E^2L^3V^8 + 48384L^2\hbar^2M^2GV^4\omega^4 + 9216\hbar M^4D\omega^8\\ &+ 2304M^4D\omega^8 + 51840\hbar^2LM^3EV^2\omega^6 + 9216\hbar^3M^4D\omega^8 - 16128\hbar^3M^2D^2L\omega^4V^4\\ &- 34560\hbar^3L^2MDEV^6\omega^2 - 34560\hbar^3L^2MDSV^4\omega^2 + 13824\hbar^2M^4D\omega^8\\ &+ 51840\hbar^2LM^3S\omega^6 + 17280\hbar LM^3EV^2\omega^6 + 17280\hbar LM^3S\omega^6\\ &+ 96768\hbar^3L^2M^2GV^4\omega^4 + 51840\hbar^3LM^3EV^2\omega^6 + 51840\hbar^3M^3LS\omega^6)\end{aligned}$$

$$\begin{aligned}\omega_6 = -\frac{\hbar LV^4}{5760M^7\omega^{12}}(&432000M^4\omega^8\hbar^4LEV^2 - 334125\hbar^4L^3V^4MS^2\omega^2 - 668250\hbar^4L^3V^6MES\omega^2\\ &- 554400\hbar^4L^3V^8MDG\omega^2 - 67200\hbar^2LV^4M^3D^2\omega^6 + 81900\hbar^5L^3V^{10}D^2E\\ &- 864000\hbar^4L^2V^6M^2ED\omega^4 - 201600\hbar^4M^3LV^4D^2\omega^6 + 43200\hbar^4LSM^4\omega^8\\ &+ 1209600L^2\hbar^4GM^3V^4\omega^6 - 864000L^2\hbar^4SM^2DV^4\omega^4 + 57600M^5\hbar^4D\omega^{10}\\ &+ 403200M^3\hbar^2L^2GV^4\omega^6 + 57600M^5\hbar D\omega^{10} + 11520M^5D\omega^{10} + 432000M^4\hbar^2LEV^2\omega^8\\ &+ 115200M^5\hbar^3D\omega^{10} - 201600L\hbar^3M^3D^2V^4\omega^6 - 432000M^2\hbar^3L^2DEV^6\omega^4\\ &- 432000M^2\hbar^3L^2DSV^4\omega^4 + 115200M^5\hbar^2D\omega^{10} + 432000M^4\hbar^2LS\omega^8\\ &+ 108000M^4\hbar LEV^2\omega^8 + 108000M^4\hbar LS\omega^8 + 1209600M^3\hbar^3L^2GV^4\omega^6\\ &+ 684000M^4\hbar^3LEV^2\omega^8 + 684000M^4\hbar^3LS\omega^8 + 35200M\hbar^4L^2D^3V^8\omega^2\\ &- 334125M\hbar^4L^3E^2V^8\omega^2 + 11520M^5\hbar^4D\omega^{10} - 554400M\hbar^5L^3GDV^8\omega^2\\ &+ 35200M\hbar^5L^2D^3V^8\omega^2 - 432000M^2\hbar^5L^2EDV^6\omega^4 - 67200M^3\hbar^5LD^2V^4\omega^6\end{aligned}$$

$$
\begin{aligned}
&- 432000M^2\hbar^5L^2SDV^4\omega^4 + 81900\hbar^5L^3D^2SV^8 + 403200M^3\hbar^5L^2GV^4\omega^6\\
&+ 10800M^4\hbar^5LEV^2\omega^8 - 334152\hbar^5L^4GEV^{10} - 334152\hbar^5L^4GSV^8\\
&- 334125M\hbar^5L^3E^2V^8\omega^2 - 668250M\hbar^5L^3ESV^6\omega^2 - 334125M\hbar^5L^3S^2V^4\omega^2\\
&+ 108000M^4\hbar^5LS\omega^8)
\end{aligned}
$$

References

[1] R.C. Batra, M. Porfiri, D. Spinello, Vibrations of narrow microbeams predeformed by an electric field, *Journal of Sound and Vibration* 309 (2008) 600–612.

[2] G.I. Taylor, The coalescence of closely spaced drops when they are at different electric potentials, *Proceedings of the Royal Society A* 306 (1968) 423–434.

[3] H.C. Nathanson, W.E. Newell, R.A. Wickstrom, J.R. Davis, The resonant gate transistor, *IEEE Transactions on Electron Devices* 14 (3) (1967) 117–133.

[4] P.M. Osterberg, Electrostatically Actuated Microelectromechanical Test Structures for Material Property Measurement, PhD Dissertation, Massachusetts Institute of Technology, 1995.

[5] V. Rochus, D.J. Rixen, J.C. Golinval, Electrostatic coupling of MEMS structures: transient simulations and dynamic pull-in, *Nonlinear Analysis* 63 (2005) e1619–e1633.

[6] S. Krylov, Lyapunov exponents as a criterion for the dynamic pull-in instability of electrostatically actuated microstructures, *International Journal of Nonlinear Mechanics* 42 (2007) 626–642.

[7] E.M. Abdel-Rahman, M.I. Younis, A.H. Nayfeh, Characterization of the mechanical behavior of an electrically actuated microbeam, *Journal of Micromechanics and Microengineering* 12 (6) (2002) 759–766.

[8] S.K. De, N.R. Aluru, Complex nonlinear oscillations in electrostatically actuated microstructures, *Journal of Microelectromechanical Systems* 15 (2) (2006) 355–369.

[9] M. Moghimi Zand, M.T. Ahmadian, Characterization of coupled-domain multi-layer microplates in pull-in phenomenon, vibrations and dynamics, *International Journal of Mechanical Sciences* 49 (11) (2007) 1226–1237.

[10] M. Moghimi Zand, M.T. Ahmadian, Vibrational analysis of electrostatically actuated microstructures considering nonlinear effects, *Communications in Nonlinear Science and Numerical Simulation* 14 (4) (2009) 1664–1678.

[11] J.H. Kuang, C.J. Chen, Dynamic characteristics of shaped micro-actuators solved using the differential quadrature method, *Journal of Micromechanics and Microengineering* 14 (4) (2004) 647–655.

[12] E.R. Konig, G. Wachutka, Multi-parameter homotopy for the numerical analysis of MEMS, *Sensors and Actuators A—Physical* 110 (2004) 39–51.

[13] A.H. Nayfeh, M.I. Younis, A new approach to the modeling and simulation of flexible microstructures under the effect of squeeze film damping, *Journal of Micromechanics and Microengineering* 14 (2004) 170–181.

[14] M.I. Younis, Modeling and Simulation of Microelectromechanical Systems in Multi-Physics Fields, PhD Dissertation, Virginia Polytechnic Institute and state University, 2004.

[15] S.J. Liao, An approximate solution technique which does not depend upon small parameters: a special example, *International Journal of Nonlinear Mechanics* 30 (1995) 371–380.

[16] S.J. Liao, *Beyond Perturbation. Introduction to Homotopy Analysis Method*, Chapman & Hall, Boca Raton, FL, 2004.

[17] S.J. Liao, A.T. Cheung, Application of homotopy analysis method in nonlinear oscillations, *ASME Journal of Applied Mechanics* 65 (1998) 914–922.

[18] S.J. Liao, An analytic approximate technique for free oscillations of positively damped systems with algebraically decaying amplitude, *International Journal of Nonlinear Mechanics* 38 (2003) 1173–1183.

[19] S. Li, S.J. Liao, An analytic approach to solve multiple solutions of a strongly nonlinear problem, *Applied Mathematics and Computation* 169 (2005) 854–865.

[20] T. Hayat, M. Sajid, On analytic solution for thin film flow of a fourth grade fluid down a vertical cylinder, *Physics Letter A* 361 (2007) 316–322.

[21] S. Abbasbandy, The application of the homotopy analysis method to nonlinear equations arising in heat transfer, *Physics Letter A* 360 (2006) 109–113.

[22] H.A. Tilmans, R. Legtenberg, Electrostatically driven vacuum-encapsulated polysilicon resonators—part II: theory and performance, *Sensors and Actuators A* 45 (1) (1994) 67–84.

[23] M. Moghimi Zand, M.T. Ahmadian, Application of homotopy analysis method in studying dynamic pull-in instability of microsystems, Mechanics Research Communications, in press, doi:10.1016/j.mechrescom.2009.03.004.